Desalination and Water Treatment
www.deswater.com
doi: 10.1080/19443994.2012.749374

51 (2013) 3497–3504
April

Taylor & Francis
Taylor & Francis Group

New low-cost composite adsorbent synthesis and characterization

Recep Akkaya[a,*], Birnur Akkaya[b]

[a]*Cumhuriyet University, Vocational School of Health Services, 58140 Sivas, Turkey*
Tel. +90 3462191010/1341; Fax: +90 3462191256; email: rakkaya@cumhuriyet.edu.tr
[b]*Department of Molecular Biology and Genetics, Faculty of Science, Cumhuriyet University, 58140 Sivas, Turkey*

Received 2 April 2012; Accepted 27 August 2012

ABSTRACT

In this research, a novel composite, poly(acrylamide-expanded perlite) [P(AAm-EP)], was synthesized and characterized. The chemical synthesis was achieved by using free-radical polymerization and a number of structural characterization methods, including Fourier-transformed infrared spectroscopy (FTIR), X-ray diffraction (XRD), Scanning Electron Microscopy (SEM), Brunauer–Emmett–Teller (BET)-porosity, and swelling tests. Free-radical polymerization of acrylamide (AAm) over expended perlite (EP) was successfully performed. The effect of reaction variables, such as dosage of the initiator, total concentration of the reactants, reactant ratio, mixing time, temperature, and reaction time, were investigated in detail. Expended perlite was cross-linked with acrylamide to enhance its chemical resistance. P(AAm-EP) composite has a specific surface area of 31.7 $m^2 g^{-1}$.

Keywords: Composite; Polyacrylamide; Chemical synthesis; Infrared spectroscopy; Expanded perlite

1. Introduction

Free-radical copolymerization, a useful technique for modifying the chemical and physical properties of natural polymers, is the most attractive method of improving expanded perlite (EP) solubility and widening its applications. Perlite, a glass-like conglomerate formed by a sudden cooling of volcanic lava, has been studied as a candidate adsorbent to be used for the removal of heavy metal ions [1–4]. Modified EP has better flocculate ability than EP itself and also has a variety of applications. This is attributed to the special molecular structure of expanded perlite. Some mechanism was presumed to have EP with moderate molecular weight and both counteracted charge and built a bridge [5,6]. Kalyani and Krishnaiah studied chitosan-coated perlite beads [7,8]; Hasan et al. synthesized a novel chitosan-coated perlite copolymer by grafting perlite onto chitosan through block copolymerization [9]; and Tekin et al. synthesized polyacrylamide (C-PAM) on EP [10].

Hydrogel polymers included within the composite compositions have often been those that retain or conduct water [11–14]. While a hydrogel by itself can be used as an adsorbent, by virtue of its functional groups, when used as the constituent of a composite, the hydrogel becomes inert [15]. The other uses of EP are for heavy metal ion removal from aqueous media [16]. Another benefit of EP application is in sludge dewatering [17]. This implies that EP is an important polymer flocculent in water treatment and sludge dewatering.

The new mechanical, electrical, photochemical, catalytic, and adsorptive properties of such composites form, in most cases, a synergic combination of individual components. Over the last few years, shape

*Corresponding author.

synthesis, consisting of a host/guest reaction, has been the most widely explored method of synthesis [18]. The synthesis of the material guest (polymer) takes place in the channels, pores, or lamina of the host structure. This process requires the careful selection of host and guest to prepare the corresponding composites. The introduction of macromolecules (i.e. polymers) into host channels confers specific properties to the resulting composites [19].

Natural adsorbents have adsorption capacities and are able to remove metal ions from wastewater at low cost. Due to their low cost and local availability and depending on their nature, adsorbents such as bentonite, zeolite, chitosan, hydroxyapatite or perlite waste products, and industry wastes are classified as low-cost adsorbents. In recent years, there has been increasing interest in finding economical and effective adsorbents such as bentonite [20], zeolite [21], chitosan [22], hydroxyapatite, [23], and perlite [24]. These adsorbents are easily available, low-cost materials with high adsorption affinities. Among these, perlite is one of the promising adsorbents for removing metal ions pollutants from wastewater. The researchers have been shown that perlite and modified perlite have an adsorption capacity for the removal of metal ions from aqueous solution [24–26]. As there are large deposits of perlite in Turkey, perlite can be easily obtained. Hence, it is a suitable low-cost adsorbent in this study that they are able to treat wastewater contaminated with metal ions by modification at low cost. The best efficiency of perlite is due to its rough structure and the presence of matrix of micro-pores in it that yields greater active surface area, enhancing adsorption.

In a previous study, a number of polyacrylamide-based composite materials were produced and used for the selective removal of heavy metal ions—UO_2^{2+}, Th^{4+}, and Pb^{2+}—from aqueous media [22,23]. The adsorptive features of these composites were studied and compared with that of other composites reported in previous works [12,22,23]. Hydrogel polymers included within the composite compositions often retain water [25–28]. Although a hydrogel by itself cannot be used as an adsorbent, when used as the constituent of a composite, the hydrogel improves the adsorptive features of the composite [29,30]. Many investigations have demonstrated that adsorbent capacity of a hydrogel can be further improved by the addition of materials with high adsorbent capacity, such as bentonite, chitosan, or zeolite [26–31], while in P(AAm-EP), P(AAm) as an inert hydrogel is enrolled as the host for the adsorbent EP. The purpose of this study was to prepare a novel affinity adsorbent [P (AAm-EP)]. In this study, P(AAm-EP) composite (with EP inside the porous channels of mesoporous materials) was synthesized by the free-radical copolymerization of acrylamide (AAm) over EP. The inert behavior of P(AAm) enables it to act as a matrix (host) within the composite, both supporting and expanding the adsorbent capacity of EP (guest) particles. It was obvious that the composite had the largest Brunauer–Emmett–Teller (BET) surface area. Large BET areas could play an important role in increasing the adsorptive capacity of a composite. The structure and surface properties of P(AAm-EP) synthesized and EP were detected and characterized with the data and analysis results obtained from Fourier transform infrared spectroscopy (FTIR), scanning electron micrograph (SEM), X-ray diffraction (XRD), BET-porosity, and swelling tests. The effects of reaction variables, such as dosage, initiator and total concentration of the reactants, reactants ratio, mixture time, temperature, and the reaction time, on free-radical polymerization were studied.

2. Experiment

2.1. Reagents

Acrylamide (monomer), N,N´-methylenebisacrylamid (crosslinking), N,N,N´,N´-tetramethylethylenediamine (TEMED) (accelerator), ammonium peroxodisulfate (initiator), ($(NH_4)_2S_2O_8$), and (APS) were obtained from Sigma Aldrich-Germany. The EP was obtained from a local source (Etibank, Izmir, Turkey). All chemicals used were of analytical reagent grade.

The mineral was first washed with water to remove fine grains and water-insoluble particles. It was then dried for 24 h at 110 °C (Table 1). Then, the dried EP samples were mechanically sieved through 100 mesh. Before each adsorption experiment, the EP

Table 1
Chemical composition of expanded perlite and physical characteristics of (EP)

Constituent	Content in mass (%)
SiO_2	73.10
Al_2O_3	14.21
Na_2O	3.12
K_2O	4.81
CaO	0.94
Fe_2O_3	1.07
MgO	0.34
Physical characteristics	*(EP)*
Particle size	100 mesh
pH	6.8
CEC (mEq/100 g)	35.1
Density (g mL^{-1})	2.3

samples were kept at 110°C for 1 h and stored in a desiccator before use.

2.2. Preparation of P(AAm-EP) Composite

Ten grams of P(AAm-EP) were synthesized through bulk polymerization in an aqueous medium (20 mL) using a 3:1 P(AAm-EP) ratio [2 g of EP and 10 mL AAm solution, containing 1/3 AAm (v/v)] [12,22,25]. In the reaction, 8 mL N,N´-methylenebisacrylamid cross-linker, 500 μg ammoniumpersulphate (APS), and 200 μL TEMED (stock solution) were used. The final reaction mixture was then stirred, using an electric agitator for 5 min at the speed of 3500 rpm min^{-1}, until the composite was completely dissolved. The reaction product, P (AAm-EP) composite, was washed in distilled water until the pH of the effluent became neutral, and the composite was then prepared to have a particle size of −25 mesh.

2.3. Characterization of the composite

The EP mineral, P(AAm), and P(AAm-EP) were characterized by FTIR, XRD, SEM, BET-porosity, and swelling studies.

The FTIR spectrometric (Mattson 1000, UK) analysis was used to characterize the chemical structure of EP, P(AAm), and P(AAm-EP). The composite and component were prepared as KBr Pellets and spectra were taken five times using 4 cm^{-1} resolution and 400–4000 cm^{-1} frequency range.

Dried particles of the EP and P(AAm-EP) were separately mounted on a sample holder of a Rigaku Dmax 2200 diffractometer equipped with Ni-filtered [2α min^{-1} scan rate, using Cu Kα radiation (λ = 1.5418 °A)], and their X-ray diffraction patterns were recorded in the range of 10–50 and at a speed of 5 min^{-1}.

The specimens of EP, P(AAm), and P(AAm-EP) were coated with a thin layer of gold under reduced pressure, and their surface morphology was visualized using 5000× and 10,000× magnification in a JEOL/JSM-6335F SEM with Tubitak/Gebze Laboratories SEM.

Specimens of EP, P(AAm), and P(AAm-EP) of similar particle size were prepared through the use of Tyler Standard sieves (Quantachrome Instruments), and their specific surface areas and micro-pore volumes were determined by a BET equation using a nitrogen adsorption system at 77 K with a Quantachromosorb Instrument. The surface area of the pure EP, P(AAm), and P(AAm-EP) micro-porous composites was also determined.

To determine the swelling behavior, 1 g of dry composite and the components was placed into distilled water and kept at 25 ± 0.5°C. Swollen specimens were periodically taken and weighed on an electronic balance. The weight ratios of dry and swollen samples were recorded. The water content of the swollen specimens was calculated using the following expression:

$$\text{Swelling ratio } (\%) = [(w_f - w_o)/w_o] \times 100$$

where w_o and w_f are the weight of the composite and component specimens, before and after swelling, respectively.

All experiments were always performed in duplicates; ±5% was the limit of experimental error of each duplicate, and any experiment resulting in a limit higher than this was repeated.

3. Results and discussion

3.1. Experimental conditions

3.1.1. Effect of the initiator and component on the production rate

The effect of the initiator was studied by changing the type of initiator. In theory, any material that can generate free radicals can initiate a polymerization reaction. The commonly used initiators are ammonium persulfate ($(NH_4)_2S_2O_8$), azo initiator ammonium, and a complex initiation system that is comprised of a mixture of the oxidant, ammonium persulfate, and reducing agent sodium sulfite. ($(NH_4)_2S_2O_8$) (Mass ratio 5:1) was used as the initiator in this experiment.

The reaction temperature was 25°C. This shows that ($(NH_4)_2S_2O_8$) was a high-efficiency initiator, and this was related to the particular trigger mechanism. Most studies use heavy metal as the initiator in free-radical copolymerization of EP. Although other types of initiators could theoretically initiate a reaction in EP, in this study, the reactions could not be initiated with them.

The effect of the total concentration of reactants (EP and P(AAm)) on the component rate have been investigated. Selections of the initiator efficiency were studied by changing the total concentration of reactants from 10% to 21%.

When the total concentration of reactants was in the range 10–21%, the embedding ratio and embedding efficiency increased; when the total concentration of reactants was increased beyond 21%, the grafting ratio and embedding efficiency decreased. Therefore, the maximum embedding rate of 32.12% and embedding efficiency of 72.42% were achieved at 13% total concentration of reactants. First, with the increase in both EP and acrylamide, the system presented a high

viscous state; thus, some raw materials could have been completely dissolved and, therefore, did not participate in the reaction.

The reaction conditions were as follows: the mass ratio of EP to acrylamide, 1:3; the reaction temperature, 25℃; percentage of initiator concentration to the total mass of the reaction system (including the aqueous solution), 0.04%; and reaction time, 4.0 h. The optimum ratio of EP to acrylamide was 3:1. The embedding rate significantly increased with the increasing mass ratio of acrylamide to EP. However, there was a slight increase in the embedding efficiency after reaching a certain degree. When the acrylamide monomer was increased, it resulted in a corresponding increase in collision opportunity between the acrylamide monomer and EP molecules, which was beneficial to the embedding of the EP macromolecules. However, the increase in acrylamide also promoted the formation of polyacrylamide, resulting in low utilization of the acrylamide monomer.

3.1.2. Effect of the reaction temperature

The higher temperature was helpful for the formation of a high polymer, but the initiation must reach a certain temperature to produce free radicals; therefore, at a temperature of 20℃, it was almost impossible for the reaction to proceed. At 25℃, the optimum polymerization efficiency was reached, but the temperature continued to rise; therefore, the embedding rate and grafting efficiency decreased. The high temperature was harmful to the stability of the active center of the acrylamide and thus reduced the free-radical initiation ability. Simultaneously, the chain transfer and the chain termination would obviously increase, enhancing homopolymerization, which hinders graft copolymerization.

3.2. Detection of the product structure

3.2.1. IR spectra of the composite

The FTIR spectra of P(AAm), EP, and P(AAm-EP) are shown in Fig. 1. The characteristic structure of the FTIR spectra of P(AAm-EP) composite (Fig. 1) shows peaks at 3,200 cm^{-1} and 3,721 cm^{-1} (≡Si–OH and =Si–2(OH)–Si–3(OH) stretching vibrations), 1,200 cm^{-1}, and 1,700 cm^{-1} (≡AI–OH and ≡AI–2(OH) stretching vibrations) due to the presence of predominant silanol groups and hydroxyl groups, respectively. In the surface hydroxyl groups, the silicon atoms at the surface tend to maintain their tetrahedral coordination with oxygen. They complete their coordination at room temperature by attachment to monovalent hydroxyl groups, forming silanol groups [17,32]. The presence of predominant silanol groups and hydroxyl groups in the composite serves as an active binding site for metals. Fig. 1 shows that there is a shift in absorption frequency of silanol groups, indicating the deformation of ≡Si=OH and ≡Si=2(OH)=Si=3(OH). This may be attributed to interaction between the functional groups and metal ions as a result of adsorption. This observation is evidence that functional groups are involved in binding the metal ions to the composite. The FTIR spectrum provides some understanding of the adsorption mechanism of metal ions by composite. This result confirms the participation of unprotonated functional groups as active binding sites for the adsorption of metals on EP. Formation of a complex between the composite and the terbium ion is shown.

3.2.2. Physical characteristics of the composite

The physical characteristics of the composite and its components are summarized in Table 1. The surface area, density, pore volume, pore diameter, and porosity of the composite and component are determined by BET instruments in Table 2. The surface area is measured by assuming that the adsorbed nitrogen forms a monolayer and possesses a molecular cross-sectional area of 31.7 $m^2 g^{-1}$. The composite has a significant difference in surface morphology between its two components. The composite was chemically bounded, which was determined by consulting the respective infrared spectroscopy charts for EP and acrylamide. Pore diameters of EP, P(AAm), and P(AAm-EP) were less than 2 nm, so all three materials could be classified as micro-porous compounds by considering IUPAC criteria.

3.2.3. X-ray diffraction (XRD) of the composite

The XRD spectroscopy of both component and composite are shown in Fig. 1. The typical EP reflections in the XRD patterns of EP and P(AAm-EP) confirmed that the main composition of the rock sample was EP. The intense increase in the background of P(AAm-EP) was due to the amorphous contribution of

Table 2
Surface morphology of EP, P(AAm), and P(AAm-EP)

Physical characteristics	(EP)	P(AAm)	P(AAm-EP)
BET/$m^2 g^{-1}$	25.2	0.42	31.7
Pore volume/$cm^3 g^{-1}$	0.12	0.01	0.14
Pore diameter/nm	0.97	0.83	0.84

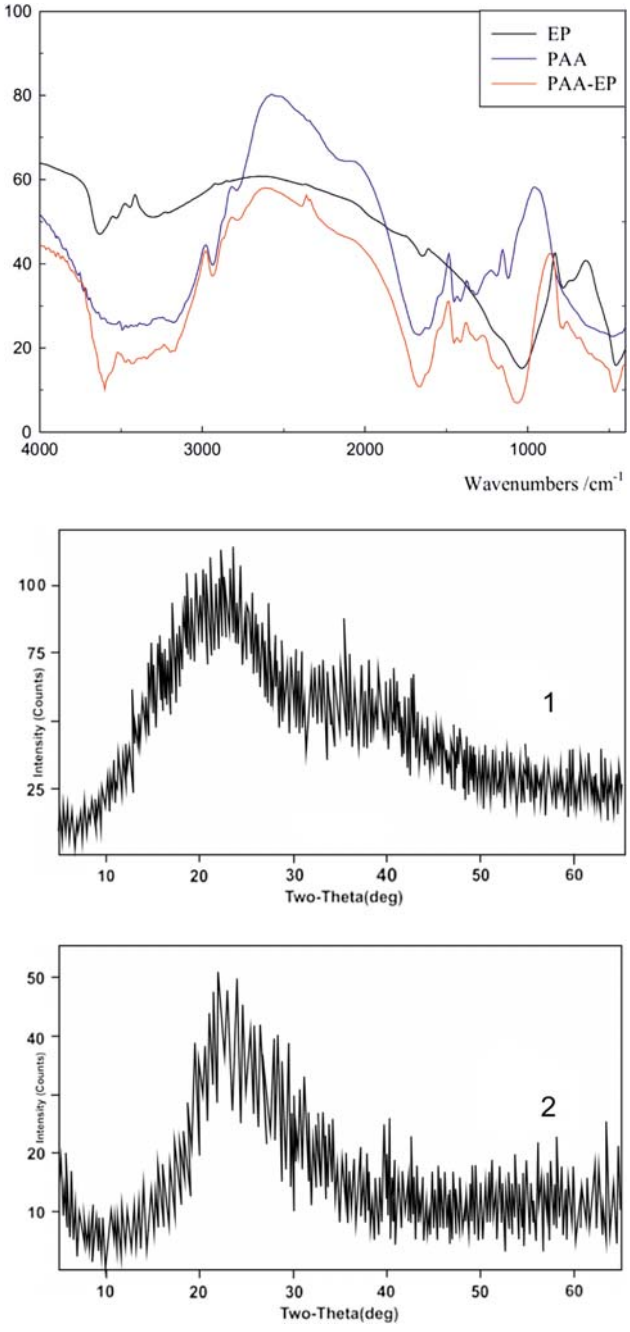

Fig. 1. Comparative FT-IR spectra of the (a) composite P (AAm-EP) and (b) its component (EP) mineral; XRD pattern of P(AAm-EP) (1) and its component pure EP mineral (2).

P(AAm) to EP. These higher background values can be attributed to the rather amorphous structure of the other component, P(AAm). This observation could also imply that the contribution of EP to the structural properties of P(AAm-EP) was minor and that the composite could be classified as a micro-composite [33,34].

3.2.4. Scanning Electron Microscopic (SEM) analysis of the composite

The SEM images of EP, acrylamide, and composite are depicted in Fig. 2. There is a significant difference in surface morphology between the two forms of each component. A striking feature of this image is the appearance of a porous internal structure in the composite. The acrylamide (Fig. 2(a)) displayed a smooth and nonporous surface while the composite

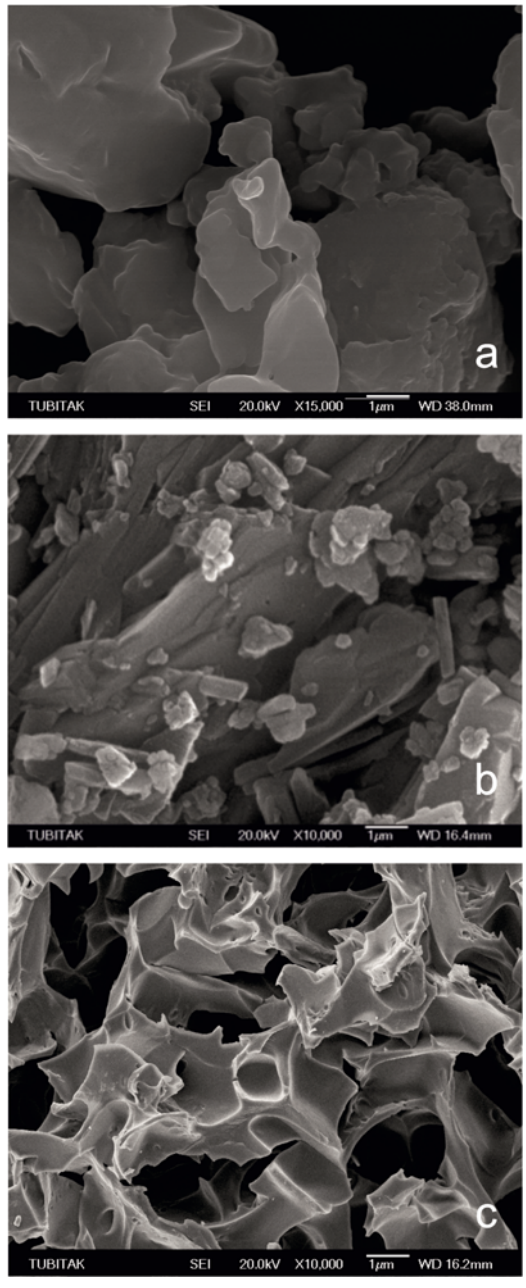

Fig. 2. SEM images of the pure (a) P(AAm), (b) EP and (c) P(AAm-EP) composite.

(Fig. 2(c)) displayed a rough and micro-porous structure, which may offer more adsorption sites for adsorption and improve the bridging ability. This result also indicated that the acrylamide has been chemically bounded, (Fig. 2(b)) which was determined by consulting an infrared spectroscopy chart for both EP and acrylamide.

3.2.5. Swelling of the composite

The EP constituted 1/3 of P(AAm-EP) (w/w). Although the water-retaining capacity of EP and P (AAm) compounds were found to be very similar, 121% and 954%, respectively, this capacity appeared to have increased by almost 100% in the composite. A hypothetical expansion value of 1457% was estimated for P(AAm-EP). This finding indicated that the combination of two less-hydrophilic compounds, EP and P (AAm), led to the formation of a very hydrophilic composite, P(AAm-EP). This large internal surface area may also provide a high ion-transfer rate. There was a slight increase for P(AAm-EP) in comparison to its individual components that might be attributed to the hydrophilic contribution of silanol groups of EP in P(AAm-EP) to P(AAm).

3.2.6. Comparasion with tradional adsorbents

The costs of adsorbents are roughly shown in Table 3. When comparing among low-cost materials, the lowest cost has been seen at perlite. Since the composite in this article consist of one-third of perlite, the cost gets considerably lower.

Here, factors affecting adsorption capacity is more important than the adsorption capacity. These essential factors are adsorbent surface area, pore size, pore structure, and active surface area [39]. High adsorption capacity and relatively high specific surface areas and more importantly, their relatively economical prices make the composite more attractive adsorbents.

Table 3
Cost of low-cost adsorbents and commercial activated carbons as reported in literature

Adsorbent	Price (US £/kg^{-1})	References
Bentonite (Montmorillonite)	0.09	[35]
Zeolite	0.12	[36]
Chitosan	0.21	[37]
Hydroxyapatite	3.3	[38]
Perlite	0.12	[36]
P(AAm-EP) composite	0.02	This study

For understanding the behavior of adsorbents, FTIR, XRD, SEM, and BET has also been carried out (Table 4). Behavior of adsorbents has been correlated with their FTIR, XRD, BET, and SEM observations. Amorphous characteristics of the composite, as indicated by XRD, also favor its characteristic feature for outstanding removal of metal ions in aquatic system. The SEM image of the composite shows cave-type openings supporting its performance. The FTIR studies confirm the presence of polar groups like silanol groups and hydroxyl groups in the composite. These polar groups help in enhancing the binding capacity of adsorbent for the metal ions. Also, the composite [P (AAm-EP)] possess good surface area due to their amorphous nature as reflected by XRD. The SEM indicates pores on surface of the composite, which are consistently distributed. These surface morphological features of the composite provide sites for better adsorption. Results clearly indicate that the composite can be used as adsorbent materials.

Table 4
The SEM and XRD observations of the adsorbent's surface

Adsorbent	SEM observations	XRD observations	BET observations (m^2/g^{-1})	References
Bentonite (Montmor.)	Needle like structural features with cave type openings	Layered	30.4	[29]
Zeolite	Loosely bound fibrous structural features	Amorphous	10.4	[12]
Chitosan	Regular features of pores, which are evenly distributed	Amorphous	1.43	[22]
Hydroxyapatite	Discrete particles of varying dimensions having smooth	Crystalline phases	17.4	[23]
Perlite	Loosely bound fibrous structural features	Amorphous	25.2	[25]
P(AAm-EP) composite	Regular features of pores, which are evenly distributed	Heterogeneous and Amorphous	31.7	This study

4. Conclusion

The inert behavior of P(AAm) enables it to act as a matrix (host) within the composite, expanding the adsorbent capacity of EP (guest) particles. In this research, a novel micro-porous composite, P(AAm-EP), was synthesized and characterized. The FTIR, XRD, SEM, and BET-porosity results collectively indicated the homogeneous formation of the P(AAm-EP) composite. The use of the mineral as a composite with P(AAm) meaningfully increased the adsorption capacities. It was obvious that the composite had the largest BET surface area ($31.7\,m^2/g^{-1}$). Large BET areas ($31.7\,m^2/g^{-1}$) could play an important role in increasing the adsorptive capacity of the composite. This composite had micro-porosity, with reference to the IUPAC classification, because its mean pore diameter value was <2 nm. The composite is a potential adsorbent for the removal of heavy metal ions from wastewater and environmental pollution. A prevention manuscript was relevant to the study of natural systems and environmental systems.

Acknowledgment

This work was supported by The Research Fund of Cumhuriyet University (CÜBAP, Project No: F-321) to which the author is grateful.

References

[1] M. Alkan, M. Dogan, Adsorption of copper (II) onto perlite, J. Colloid. İnterf. Sci. 243 (2001) 280–291.
[2] M. Doğan, M. Alkan, Adsorption kinetics of methyl violet onto perlite, Chemosphere 50 (2003) 517–528.
[3] M. Alkan, Ö. Demirbas, M. Dogan, Zeta potential of unexpanded and expanded perlite in various electrolyte media, Micropor. Mesopor. Mat. 84 (2005) 192–200.
[4] Z. Talip, M. Eral, U. Hiçsonmez, Adsorption of thorium from aqueous solutions by perlite, J. Environ. Radioactive. 100 (2009) 139–143.
[5] M. Alkan, M. Dogan, Some physicochemical properties of perlite as an adsorbent, Fresen. Environ. Bull. 13 (2003) 251–257.
[6] A. Sari, A. Karaipekli, Fatty acid esters-based composite phase change materials for thermal energy storage in buildings, Appl. Therm. Eng. 37 (2012) 208–216.
[7] S. Kalyani, J.A. Priya, P.S. Rao, A. Krishnaiah, Removal of copper and nickel from aqueous solutions using chitosan coated on perlite as bio sorbent, Sep. Sci. Technol. 40 (2005) 1483–1495.
[8] S. Kalyani, A. Krishnaiah, Adsorption of divalent cobalt from aqueous solution onto chitosan–coated perlite beads as biosorbent, Sep. Sci. Technol. 42 (2007) 2767–2786.
[9] S. Hasan, A. Krishnaiah, T.K. Ghosh, D.S. Viswanath, V.M. Boddu, E.D. Smith, Adsorption of chromium (VI) on chitosan-coated Perlite, Sep. Sci. Technol. 38 (2003) 3775–3793.
[10] N. Tekin, A. Dinçer, Ö. Demirbaş, M. Alkan, Adsorption of cationic polyacrylamide (C-PAM) on expanded perlite, App. Clay Sci. 50 (2010) 125–129.
[11] H. Kasgoz, A. Durmus, A. Kasgoz, Enhanced swelling and adsorption properties of AAm-AMPSNa/clay hydrogel nanocomposites for heavy metal ion removal, Polym. Adv. Technol. 19 (2008) 213–220.
[12] R. Akkaya, Preparation of Bentonite/Zeolite-Polyhdroxyethyl Methacrylate and Polyacrylamide-co-Maleic acid Composites and Investigation Fort Their Adsorptive Features for Metal Ions, Ph.D. Thesis, Cumhuriyet University, Sivas, Turkey, 2009, pp. 1–158.
[13] J. Yun, D. Jin, Y. Lee, H. Kim, Photocatalytic treatment of acidic waste water by electrospun composite nanofibers of pH-sensitive hydrogel and TiO_2, Mater. Lett. 64 (2010) 2431–2434.
[14] Z. Weian, L. Wei, F. Yue, Synthesis and properties of a novel hydrogel nanocomposites, Mater. Lett. 59 (2005) 2876–2880.
[15] T.S. Anirudhan, P.S. Suchithra, Heavy metals uptake from aqueous solutions and industrial wastewaters by humic acid-immobilized polymer/bentonite composite: Kinetics and equilibrium modelling, Chem. Eng. J. 156 (2010) 146–156.
[16] F. Aydin, F. Yasar, I. Aydin, F. Guzel, Determination of lead separated selectively with ion exchange method from solution onto BCW in Sirnak, East Anatolia of Turkey, Microchem. J. 98 (2011) 246–253.
[17] T. Mathialagan, T. Viraraghavan, Adsorption of cadmium from aqueous solutions by perlite, J. Hazard. Mater. 94 (2002) 291–303.
[18] S. Kawi, A high-surface-area silica–clay composite material, Mater. Lett. 38 (1999) 351–355.
[19] M.L. Martinez, F.A.L. D'Amicis, A.R. Beltramone, M.B.G. Costa, O.A. Anunziata, Synthesis and characterization of new composites: PANI/Na-AlSBA-3 and PANI/Na-AlSBA-16, Mater. Res. Bul. 46 (2011) 1011–1021.
[20] B. Akkaya, IgG purification by bentonite–acrylamide–histidine microcomposite, Colloid. Surface: B 92 (2012) 151–155.
[21] U. Ulusoy, S. Simsek, Lead removal by polyacrylamide-bentonite and zeolite composites: Effect of phytic acid immobilization, J. Hazard. Mater. 127 (2005) 163–171.
[22] R. Akkaya, U. Ulusoy, Adsorptive features of chitosan entrapped in polyacrylamide hydrogel for Pb^{2+}, UO_2^{2+} and Th^{4+}, J. Hazard. Mater. 151 (2008) 380–388.
[23] U. Ulusoy, R. Akkaya, Adsorptive features of polyacrylamide–apatite nanocomposite for Pb^{2+}, UO_2^{2+} and Th^{4+}, J. Hazard. Mater. 163 (2009) 98–108.
[24] Akkaya R, Effects of pH, concentration and temperature on radionuclides sorption onto polyhydroxyethyl methacrylate-expanded perlite. J. Radioanal. Nuc. Chem. 2012; doi:10.1007/s10967-012-1868-x.
[25] R. Akkaya, Removal of radionuclides of the U- and Th- series from aqueous solutions by adsorption onto Polyacryamide-expanded perlite: Effects of pH, concentration and temperature, Nucl. Inst. Method. Phy. Res. A. 688 (2012) 80–83.
[26] R. Akkaya, Synthesis and characterization of a new low-cost composite for the adsorption of rare earth ions from aqueous solutions, Chem. Eng. J. 200–202 (2012) 186–191.
[27] R. Akkaya, Thermodynamic parameters of Tl^{+}, Ra^{2+}, Bi^{3+} and Ac^{3+} adsorption onto polyhydroxyethylmethacrylate-hydroxyapatite composite, J. Radioanal. Nucl. Chem. 292 (2012) 771–775.
[28] Akkaya R, Synthesis and Characterization of Poly (2-hydroxyethylmethacrylate-hydroxyapatite) a Novel Composite for the Removal of Lead(II) from Aqueous Solutions. Clean – Soil, Air, Water 40 (2012) 1257–1264.
[29] Akkaya B, Akkaya R, Cross-linked bentonite-acrylamide-histidine-based metal-chelate affinity microcomposites for lysozyme separation from egg white. Sep. Sci. Technol. (2012). doi:10.1080/01496395.2012.683124.
[30] B. Akkaya, R. Akkaya, A crosslinked carboxylic acid containing cation exchange monolithic cryogel for human serum albumin separation, J. Macromol. Sci. A. 49 (2012) 736–743.
[31] Akkaya R. Separation of uranium and thorium in aqueous solution using polyhydroxyethylmethacrylate-hydroxyapatite novel composite. Desalin. Water Treat. (2012). doi: 10.1080/19443994.2012.708566.

[32] H. Ghassabzadeha, A. Mohadespourb, M. Torab-Mostaedic, P. Zaherib, M.G. Maraghehc, H. Taheric, Adsorption of Ag, Cu and Hg from aqueous solutions using expanded perlite, J. Hazard. Mater. 177 (2010) 950–955.
[33] A. Dyer, S. Tangkawanit, K. Rangsriwatananon, Exchange diffusion of Cu^{2+}, Ni^{2+}, Pb^{2+} and Zn2+ into analcime synthesized from perlite, Micropor. Mesopor. Mat. 75 (2004) 273–279.
[34] G. Vijayakumar, M. Dharmendirakumar, S. Renganathan, S. Sivanesan, G. Baskar, K.P. Elango, Removal of congo red from aqueous solutions by perlite, Chem. Eng. J. 37 (2009) 355–364.
[35] M.D. Ahmaruzzaman, Adsorption of phenolic compounds on low-cost adsorbents, Adv. Colloid Interface Sci. 143 (2008) 48–67.
[36] D.W. Breck, Zeolite Molecular Sieves, Structure, Chemistry and Use, John Wiley & Sons, Inc., New York,. by Krieger, Malabar, Florida, 1984. 1974.
[37] M. Dinesh, U. Charles, J. Pittman, Arsenic removal from water/wastewater using adsorbents—a critical review, J. Hazard. Mater. 142 (2007) 1–53.
[38] A. Salem, R. Akbari, Removal of lead from solution by combination of natural zeolite–kaolin–bentonite as a new low-cost adsorbent, Chem. Eng. J. 174 (2011) 619–628.
[39] C.P. Kaushik, T. Ravinder, J. Namrata Kaushik, K. Sharma, Minimization of organic chemical load in direct dyes effluent using low cost adsorbents, Chem. Eng. J. 155 (2009) 234–240.